Electric-Field-Driven Nanosecond Ferroelastic-Domain Switching Dynamics in Epitaxial Pb(Zr,Ti)O₃ Film

Hyeon Jun Lee,[1,†] Takao Shimizu,[2] Hiroshi Funakubo,[2] Yasuhiko Imai,[3] Osami Sakata,[4] Seung Hyun Hwang,[1]
Tae Yeon Kim,[1] Changjae Yoon,[1] Cheng Dai,[5] Long Q. Chen,[5] Su Yong Lee,[6] and Ji Young Jo[1,*]

[1]*School of Materials Science and Engineering, Gwangju Institute of Science and Technology, Gwangju 61005, South Korea*
[2]*Department of Materials Science and Engineering, School of Materials and Chemical Technology,*
Tokyo Institute of Technology, Tokyo 152-8550, Japan
[3]*SPring-8, Japanese Synchrotron Radiation Research Institute, Hyogo 679-5198, Japan*
[4]*Synchrotron X-ray Group, Research Center for Advanced Measurement and Characterization,*
National Institute for Materials Science, Hyogo 679-5148, Japan
[5]*Department of Materials Science and Engineering, Pennsylvania State University, Pennsylvania 16802, USA*
[6]*Pohang Accelerator Laboratory, Pohang University of Science and Technology, Pohang 37676, South Korea*

Epitaxial oxide ferroelectric films exhibit emerging phenomena arising from complex domain configurations even at pseudoequilibrium, including the creation of domain states unfavored in nature and abrupt piezoelectric coefficients around morphotropic phase boundaries. The nanometer-sized domain configurations and their domain switching dynamics under external stimuli are directly linked to the ultrafast manipulation of ferroelectric thin films; however, complex domain switching dynamics under homogeneous electric fields has not been fully explored, especially at the nanosecond timescale. This Letter reports the nanosecond dynamics of ferroelastic-domain switching from the 90° to 180° direction using time-resolved x-ray microdiffraction under homogeneous electric fields onto an epitaxial Pb(Zr$_{0.35}$, Ti$_{0.65}$)O₃ film capacitor. It is found that the application of electric fields induces spatially heterogeneous domain switching processes via intermediate domain structures with rotated polarization vectors. In addition, the domain switching time is shown to be inversely proportional to the magnitude of the applied electric field, and electric fields higher than 480 kV/cm are found to complete the ferroelastic switching within nanoseconds.

In epitaxial oxide thin films, the competition between elastic and electrostatic energy leads to complex polarization topologies, such as vortices [1,2], stripe domains [3], and 90° domain walls [4–6] in ferroic material systems. The fundamental understanding of complex domain switching dynamics under external electric fields, which is the same operation condition for electrical devices, is key to manipulating logic states connected to the overall domain configuration at nanosecond timescales. Thermodynamic calculations have predicted the application of electric fields can switch exotic domains to the same direction parallel to the electric field, accompanied by a change in the energy landscape in the thin film [7,8]. Recent dynamical calculations have predicted that the subsound velocity of domain walls enables polarization switching within a few nanoseconds [9,10]. Few experimental studies based on *in situ* microscopies and x-ray diffraction methods have probed the domain reconfiguration in ferroelectric heterostructures under the application of an electric field; however, because of existing experimental limitations such as slow electrical charging from tip-induced localized fields and/or poor temporal resolutions, the switching dynamics on those

timescales has not been fully explored to address the critical question: how fast can exotic domains be switched under electric fields [11–16].

Ferroelastic domains, which are smaller than a few nanometers with a different polarization direction in comparison to matrix domains [4], allow us to understand the ultrafast domain switching dynamics of ferroic materials. Ferroelastic switching from 90° domain walls to 180° domains along the electric-field direction occurs through the rotation of polarization and consequent growth of domains along the lateral direction. Investigating how much and how fast 90° domains rotate under the application of homogenous electric fields is fundamental for the time-dependent switching behavior of ferroelastic domains to a homogeneous domain without any spatial distribution, which is directly linked to the operation of devices based on ferroic materials. Here, we report the ultrafast ferroelastic switching dynamics of Pb(Zr$_{0.35}$Ti$_{0.65}$)O₃ (PZT) films under homogenous electric fields using the time-resolved x-ray microdiffraction (TRXμD) technique [16], which employs an x-ray pulse probe with a duration of 100 ps and a diameter of 5 μm. It allows us to monitor

individual reflections arising from a and c domains on the timescale of 100 ps. We applied homogenous electric pulses with a duration of a few nanoseconds to capacitor media and simultaneously recorded the scattered x-ray intensities in reciprocal space using a two-dimensional (2D) pixel array detector. By reconstructing the reciprocal space map (RSM) from captured scattered x rays, we show that the applied electric field can distort the reciprocal space of the ferroelectric film, accompanied by the rotation of polarization in a domains and adjacent domains. We also show that the application of a higher magnitude of electric field can result in the faster switching of ferroelastic domains even in nanoseconds.

In $Pb(Zr, Ti)O_3$ (PZT) thin films, it has been well known that ferroelastic a domains coexist with ferroelectric c domains with an orthogonal crystallographic orientation [17]. The switching dynamics of a domains under orthogonal electric fields has been a question from scientific as well as technological points of view. However, the instability of ferroelectric thin films such as the exponential increase in leakage current density under the electric field has limited experimental studies on ferroelastic a-domain switching under a homogeneous electric field with a sufficiently high amplitude for switching from the a domain to the c domain [18]. In order to suppress the instability of the thin film under a homogeneous electric field as well as investigate the switching of a and c domains in PZT films, we used the TRXμD technique. We applied an electric field (E) to a 250-nm-thick PZT thin film capacitor. A microsized x-ray beam was focused onto the capacitor within which we could investigate the ferroelastic switching as well as crystallographic behaviors.

The 250-nm-thick PZT film was grown on a $SrRuO_3/SrTiO_3$ substrate using chemical vapor deposition. The Pt top electrodes with a diameter of 100 μm were fabricated in order to apply electric field to the PZT film along the normal direction of the surface. TRXμD was conducted at beam line BL13XU at the SPring-8 synchrotron. At Spring-8, a photon beam with an energy of 12.3 keV was focused to a spot with a size of 5 μm using a refractive lens. Diffraction patterns were accumulated while thousands of electric pulses were applied to achieve sufficient diffracted x-ray intensity. Diffracted x rays from the sample were acquired using a gated pixel array detector (Pilatus 100K, Dectris Ltd.).

The RSM in Fig. 1(a) directly shows crystallographic information of a and c domains in the PZT capacitor, including lattice parameters, crystallographic orientations, and volume fractions of individual domains. This RSM was measured after the application of a few electric pulses and different from the RSM of as-grown state, as shown in Fig. S1(a) (see Supplemental Material [19]). We find two distinct reflection peaks near $Q_Z = 3.04$ and 3.16 Å^{-1} at $Q_X \neq 0$ in addition to a weak reflection at $Q_Z = 3.043$ Å^{-1} and $Q_X = 0$ (here, Q_Z and Q_X represent scattering wave
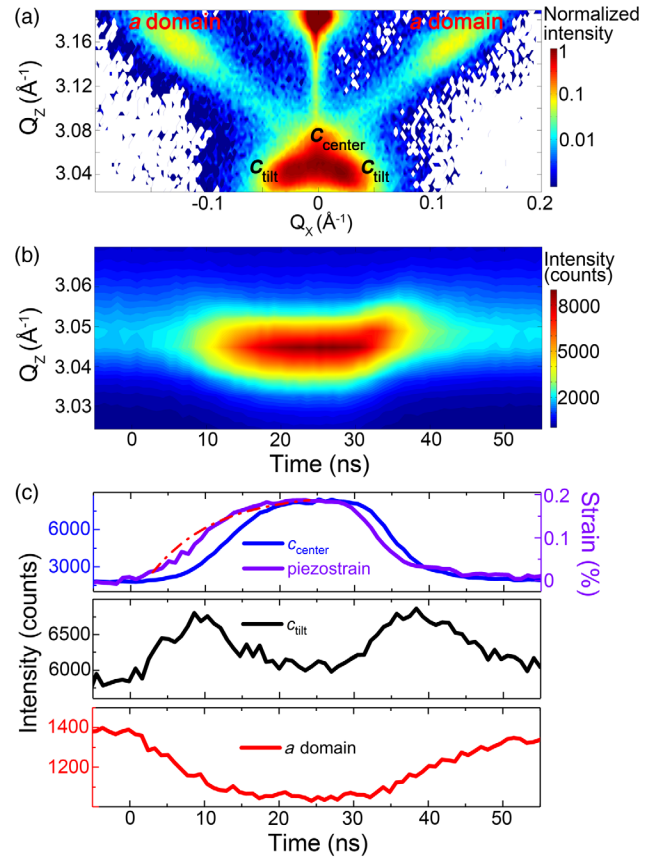

FIG. 1. (a) Reciprocal space maps (RSMs) of diffracted intensity as a function of Q_X and Q_Z near the (002) reflection from c domains and (200) reflection from a domains in 250-nm-thick PZT thin-film capacitor. (b) Evolution of PZT (002) reflection at $Q_X = 0$ as a function of time during the application of an electric field with a magnitude of 360 kV/cm and duration of 30 ns. (c) Time dependence of domain reflections from c_{center} domains at $Q_X = 0$ (top panel), c_{tilt} domains at $Q_X = 0.025$ Å^{-1} (middle panel), and a domains at $Q_X = 0.1$ Å^{-1} (bottom panel). Both the lattice parameters and intensities were acquired from the central position of the Q_z (scattering wave vector) curves, fitted using the Gaussian distribution function. The red dash-dotted line in the top panel indicates a fitted curve for the evolution of piezoelectric strain as a function of time using an exponential decay function with time constant (τ) of 9 ns.

vectors along the *out-of-plane* direction and *in-plane* direction of the PZT film, respectively). The reflection peaks at $Q_Z = 3.04$ and 3.043 Å^{-1} correspond to a PZT (002) reflection from tilted c domains from the surface normal direction (c_{tilt}) and c domains parallel to the surface normal direction (c_{center}), respectively, while the PZT (200) reflection at $Q_Z = 3.16$ Å^{-1} arises from a domains. Tensile internal stress, arising from the structural phase transition from cubic to tetragonal phase below the Curie temperature, can be relaxed through the formation of $a/c_{tilt}/a/c_{tilt}$ twin domain in the PZT film. The weak diffracted intensity from the c_{center} domain reveals the existence of a thin monodomain layer without twin domains. The estimated
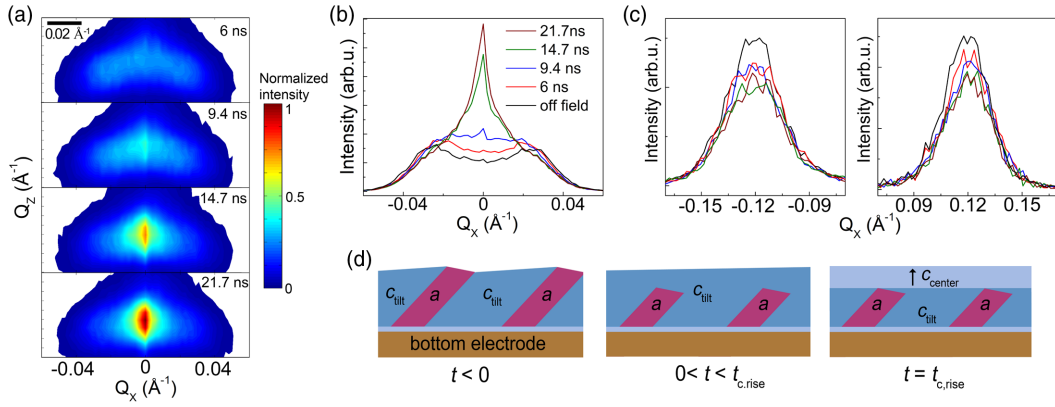
FIG. 2. (a) Reconstructed RSMs from c domains depending on the elapsed time during the application of an electric field on the film. (b) and (c) Reflected x-ray intensities along the in-plane direction near reflection for c and a domains, respectively, as a function of elapsed time. (d) Schemes for domain configuration with the elapsed time under the E (left) before the E, (middle) intermediate state during the evolution, and (right) after the characteristic time to reach 80% of the maximum intensity. A thin layer near the interface at all three schemes indicates the c_{center} domain initially formed due to the high strain field near dislocations.

a- and c-axis lattice parameters from the PZT (200) reflection and PZT (002) reflection are 3.989 and 4.133 Å under a zero-electric field ($E = 0$), respectively. Our c-axis lattice parameter for c domains of the PZT film is similar to that of bulk PZT [20], indicating that the misfit strain in the PZT film is nearly zero. The Q_X value of the reflections of the c_{tilt} and a domains can quantitatively indicate that the tilting angles of a domains (θ_a) and c_{tilt} domains (θ_c) from the surface normal direction are 1.33° and 0.26°, respectively. The estimated volume fraction of c_{tilt} domains (V_c) using the analytic equation of $V_c = \theta_a/(2\theta_c + \theta_a)$ is approximately 67%, which is similar to the estimated value based on Landau-Ginzburg-Devonshire theory with the assumption of zero misfit strain in the PZT film [8,21]. Figure S1(b) shows a real space map around the reflection from c_{tilt} domains at $t < 0$ and during the application of E, respectively (see Supplemental Material [19]). Under the application of E, the increase in diffracted intensity from the (002) reflection indicates a homogeneous increase in the amount of c_{center} domains within the capacitor.

We monitored the time-dependent evolution of individual domain reflection to probe the ultrafast ferroelastic switching dynamics using the TRXμD experiment with a combination of E pulses and x-ray pulses. Figures 1(b) and 1(c) show that the c-axis lattice parameter increases owing to the piezoelectric expansion of the PZT film and that the diffracted intensity of c_{center} domains dramatically changes under an electric square pulse with a magnitude of 360 kV/cm and a duration of 30 ns. The time constant (τ) of the rising edge for strain evolution based on an exponential decay fitting function, related to the charging time of a capacitor (RC time), is evaluated to be 9 ns. Meanwhile, the diffracted intensity from c_{center} domains begins to increase after 5 ns with respect to the beginning of piezoelectric strain. The measured piezoelectric coefficient of c_{enter} domains is 50 pm/V. In contrast, the measured

piezoelectric coefficients of both c_{tilt} and a domains are less than 10 pm/V. Under the application of an electric pulse, the diffracted intensity from a domains gradually decreases. When a characteristic time is defined by a time to reach 80% of maximum or minimum intensity under the E, the characteristic time for c_{center} domains ($t_{c,rise}$) is 15.7 ns, which is even longer than the characteristic time of 9.8 ns for a domains ($t_{a,rise}$). Unlike gradual changes in diffraction intensities from c_{center} and a domains, the diffracted intensity of c_{tilt} domains reaches a maximum of about 10 ns and then decreases.

In order to understand the time-dependent intensities and peak position of reflections, we reconstructed the time-dependent three-dimensional reciprocal space by taking the RSM obtained using a 2D x-ray detector. The RSM at various delay times, as shown in Fig. 2(a), apparently indicates two important features. (1) In (002) reflection for c_{tilt} domains; the Q_X position decreases and the intensity increases simultaneously even before the RC time (9 ns), as shown in Figs. 2(a) and 2(b). Meanwhile, the a domains show the decreased diffraction intensity without a significant change in Q_X position, as shown in Fig. 2(c). As the mean width of the domain is inversely proportional to the tilting angle [21], the conserved tilting angle of a domains with the decreased diffraction intensities as a function of elapsed time indicates a decrease in volume fraction of a domains along the *out-of-plane* direction rather than *in-plane* direction. (2) After the RC time (9 ns), the PZT (002) reflection exhibits an abrupt increase in intensity at $Q_X = 0$, which can be clearly distinguished from reflections arising from c_{tilt} domains located at $Q_X \neq 0$. The increase in intensity of the reflection from the c_{center} domains indicates ferroelastic switching along the *out-of-plane* direction, resulting in the formation of only c domains in the PZT film, unlike the $a/c/a/c$-type configuration.
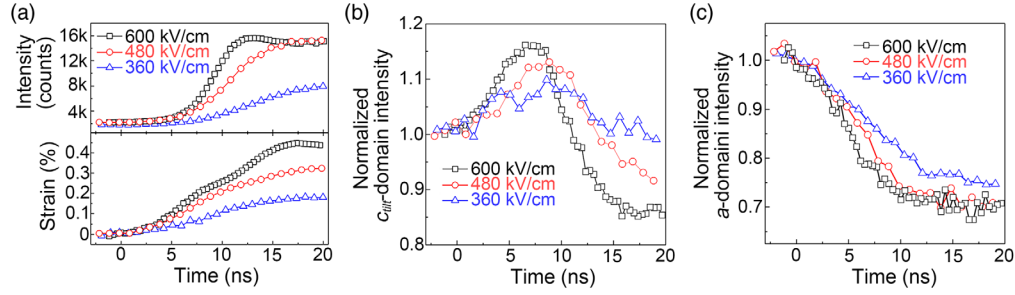
FIG. 3. (a) (top panel) Time dependence of intensities of diffracted x rays from (002) reflections at $Q_x = 0$ and (bottom panel) strain along the *out-of-plane* direction of the film under $E = 360$, 480, and 600 kV/cm. Time dependence of normalized intensities near (b) c_{tilt} domain reflection and (c) (200) reflections from a domains.

We hypothesized a heterogeneous domain switching model to account for ferroelastic switching from a to c_{center} domains via intermediate c_{tilt} domains under electric fields along the [001] direction. We assumed strongly bounded a domains at dislocations near the interface, as recently reported by a transmitted electron microscopy study, which is in excellent agreement with our phase-field simulation under a homogeneous field (Fig. S2, see Supplemental Material [19]). Before the RC time, partial a domains can be initially switched to c_{tilt} domains without the formation of c_{center} domains, as shown in Fig. 2(d). Theoretically, the switching of a domains can occur within 3 ns at $E = 360$ kV/cm when the calculated speed of domain wall motion is 3.3 m/s [9]; however, the intrinsic switching time from a to c_{tilt} domains has been experimentally unclear. After the most a domains have been switched to the c_{tilt} domains within the RC time, additional switching of these c_{tilt} domains to c_{center} domains occurs within 6 ns at $E = 360$ kV/cm. Considering that the intrinsic timescale for polarization rotation is approximately a few picoseconds [9,22,23], the nanosecond switching time indicates that the domain growth is a slower process for hindering the switching from c_{tilt} domains to c_{center} domains.

As domain growth is the dominant process for consequent ferroelastic switching [24], the higher E can provide a faster timescale to complete the ferroelastic switching. As shown in the top panel of Fig. 3(a), we find that the $t_{c,\text{rise}}$ of c_{center} domains reaches down to 13 and 10 ns at $E = 480$ and 600 kV/cm, respectively. We also find that higher E than 360 kV/cm induces a larger change in intensity from c_{center} domains, directly indicating the more energetically favored c_{center} configuration. The strain value linearly increases up to the maximum as a function of E, as shown in the bottom panel of Fig. 3(a), indicating that there is no electrical breakdown up to $E = 600$ kV/cm. The time to reach the maximum intensity of c_{tilt} domains resulting from heterogeneous domain switching, as shown in Fig. 3(b), becomes shorter under the higher E. Figure 3(c) also clearly shows the more rapid decrease in diffraction intensities of the a domain at higher E, indicating the faster ferroelastic switching from a to c_{tilt} domains. The evaluated $t_{a,\text{rise}}$ at

$E = 480$ and 600 kV/cm is 8.3 and 7.0 ns, respectively. The similar value of diffracted intensities from c_{center} and a domains at 15 ns with $E = 460$ and 600 kV/cm can be considered to be due to all the switchable a domains in the capacitor completely switching to c_{center} domains.

A subsequent reconfiguration from c_{center} to a domains occurs after turning off E at the end of the applied pulse (t_{off}). Simultaneous changes in diffracted intensities from all the reflections, as shown in Figs. 4(a), 4(b), and 4(c), show the structural recovery from the c_{center} domain to the a domain via the intermediate c_{tilt} domain. Immediately after turning off E, we find that the intensities for c_{center} domains decrease, and it takes 8.7 ns from t_{off} for the maximum intensity to reduce by 80% from the c_{center} domains ($t_{c,\text{fall}}$). The diffracted intensity from c_{tilt} domains gradually increases up to 10 ns after turning off E and then returns to the initial intensity corresponding to $t < 0$. We also find that the intensities for a domains gradually increase, and it takes 16.5 ns for the maximum intensity to reduce by 80%
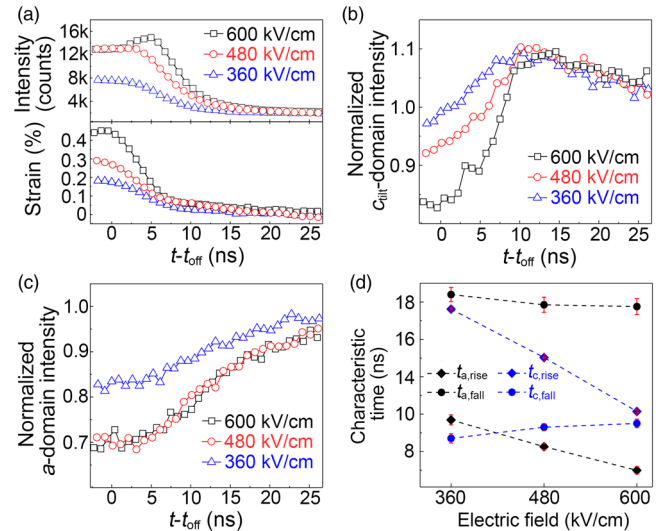

FIG. 4. (a) (Top panel) diffracted intensities and (bottom panel) time-dependent strain of c_{center} domains. Normalized intensities from (b) c_{tilt} domains and (c) a domains as a function of elapsed time after t_{off}. (d) Characteristic times for the domain reflections as a function of the magnitude of the applied electric field.

from the a domains ($t_{a,\text{fall}}$), indicating that the reconfiguration process of ferroelastic domains is even slower than the switching process from a to c domains. The $t_{c,\text{fall}}$ and $t_{a,\text{fall}}$ at $E = 680$ kV/cm are measured to be 9.5 and 15.8 ns, respectively, indicating that the time for the reconfiguration of ferroelastic domains weakly depends on the magnitude of E. In contrast to the decreased potential energy for the ferroelastic switching from a to c domains with the application of E, the weak E dependence of the reconfiguration of ferroelastic domains can be attributed to an equivalent energy landscape after turning off E [8,13].

In summary, we investigated the ultrafast ferroelastic-domain switching dynamics from a domains to c domains under a homogeneous electric field using TRXμD. The time-dependent RSM revealed that the external electric field can induce ferroelastic switching from a to c_{center} domains via intermediate c_{tilt} domains within tens of nanoseconds. With the increase in magnitude of E, the characteristic time to complete ferroelastic switching from the a to c domains proportionally decreases. We also found that the $t_{c,\text{rise}}$ is almost the same as the RC time, suggesting that the development of capacitor geometry can facilitate faster domain switching within a timescale down to the intrinsic polarization switching time. We successfully demonstrated that ferroelastic switching can be manipulated at a timescale down to the nanosecond, with which the ferroelastic a/c domain configuration can be critical for electronic applications beyond the GHz region.

*Corresponding author.
jyjo@gist.ac.kr
†Present address: Department of Materials Science and Engineering, University of Wisconsin Madison, Madison, Wisconsin 53706, USA.

[1] A. R. Damodaran *et al.*, Nat. Mater. **16**, 1003 (2017).
[2] Z. Hong *et al.*, Nano Lett. **17**, 2246 (2017).
[3] P. Zubko, N. Stucki, C. Lichtensteiger, and J. M. Triscone, Phys. Rev. Lett. **104**, 187601 (2010).
[4] V. Nagarajan, A. Roytburd, A. Stanishevsky, S. Prasertchoung, T. Zhao, L. Chen, J. Melngailis, O. Auciello, and R. Ramesh, Nat. Mater. **2**, 43 (2002).
[5] G. Catalan, A. Lubk, A. H. G. Vlooswijk, E. Snoeck, C. Magen, A. Janssens, G. Rispens, G. Rijnders, D. H. A. Blank, and B. Noheda, Nat. Mater. **10**, 963 (2011).
[6] Y. Liu, Y.-J. Wang, Y.-L. Zhu, C.-H. Lei, Y.-L. Tang, S. Li, S.-R. Zhang, J. Li, and X.-L. Ma, Nano Lett. **17**, 7258 (2017).
[7] J. Wang, S.-Q. Shi, L.-Q. Chen, Y. Li, and T.-Y. Zhang, Acta Mater. **52**, 749 (2004).
[8] E. P. Houwman, K. Vergeer, G. Koster, and G. Rijnders, in *Correlated Functional Oxides: Nanocomposites, and Heterostructures*, edited by H. Nishikawa *et al.* (Springer International Publishing, Cham, 2017), p. 29.
[9] S. Liu, I. Grinberg, and A. M. Rappe, Nature (London) **534**, 360 (2016).
[10] H. Akamatsu *et al.*, Phys. Rev. Lett. **120**, 096101 (2018).
[11] J. C. Agar *et al.*, Nat. Mater. **15**, 549 (2016).
[12] P. Gao *et al.*, Nat. Commun. **5**, 3801 (2014).
[13] A. I. Khan, X. Marti, C. Serrao, R. Ramesh, and S. Salahuddin, Nano Lett. **15**, 2229 (2015).
[14] S. M. Yang, J. Y. Jo, D. J. Kim, H. Sung, T. W. Noh, H. N. Lee, J. G. Yoon, and T. K. Song, Appl. Phys. Lett. **92**, 252901 (2008).
[15] Y. Ehara *et al.*, Sci. Rep. **7**, 9641 (2017).
[16] J. Y. Jo, P. Chen, R. J. Sichel, S. J. Callori, J. Sinsheimer, E. M. Dufresne, M. Dawber, and P. G. Evans, Phys. Rev. Lett. **107**, 055501 (2011).
[17] K. Saito, T. Kurosawa, T. Akai, T. Oikawa, and H. Funakubo, J. Appl. Phys. **93**, 545 (2003).
[18] A. Grigoriev, R. Sichel, H. N. Lee, E. C. Landahl, B. Adams, E. M. Dufresne, and P. G. Evans, Phys. Rev. Lett. **100**, 027604 (2008).
[19] See Supplemental Material at http://link.aps.org/supplemental/10.1103/PhysRevLett.123.217601 for more detailed discussion of the real space mapping, crystal structure, and phase field simulation.
[20] H. R. Johannes Frantti, J. Lappalainen, S. Eriksson, V. Lantto, S. Nishio, M. Kakihana, and S. Ivanov, Jpn. J. Appl. Phys. **39**, 5697 (2000).
[21] S. Utsugi, T. Fujisawa, R. Ikariyama, S. Yasui, H. Nakaki, T. Yamada, M. Ishikawa, M. Matsushima, H. Morioka, and H. Funakubo, Appl. Phys. Lett. **94**, 052906 (2009).
[22] R. Mankowsky, A. von Hoegen, M. Först, and A. Cavalleri, Phys. Rev. Lett. **118**, 197601 (2017).
[23] F. Chen, Y. Zhu, S. Liu, Y. Qi, H. Y. Hwang, N. C. Brandt, J. Lu, F. Quirin, H. Enquist, P. Zalden *et al.*, Phys. Rev. B **94**, 180104(R) (2016).
[24] J. Y. Jo, S. M. Yang, T. H. Kim, H. N. Lee, J. G. Yoon, S. Park, Y. Jo, M. H. Jung, and T. W. Noh, Phys. Rev. Lett. **102**, 045701 (2009).